

**POLYHYDROXYALKANOATES PRODUCTION
BY *Cupriavidus necator* MUTANTS FROM
GLUCOSE BY INNOVATIVE FERMENTATION
STRATEGIES**

NAZILA BIGLARI

UNIVERSITI SAINS MALAYSIA

2020

**POLYHYDROXYALKANOATES PRODUCTION
BY *Cupriavidus necator* MUTANTS FROM
GLUCOSE BY INNOVATIVE FERMENTATION
STRATEGIES**

by

NAZILA BIGLARI

**Thesis submitted in fulfilment of the requirements
for the degree of
Doctor of Philosophy**

January 2020

ACKNOWLEDGEMENT

First and foremost, I owe my deepest gratitude to my supervisor, Prof. Dr. K. Sudesh Kumar for his guidance, encouragement, and constructive feedback during my PhD study. I offer my sincerest thanks to Ecobiomaterial Research Laboratory members (Lab 409) who helped me during my PhD journey. I also offer my regards and blessings to all my lovely friends who stood by me during tough time; supported and helped me to complete this thesis. I am also particularly grateful to the respected Dean, Prof. Dr. Amirul Al-Ashraf Abdullah, Deputy Dean of Research, Prof. Dr. Latiffah Zakaria, Deputy Dean of Academic, Associate Prof. Dr. Asyraf Mansor, and staff from School of Biological Sciences. I am also grateful to Prof. Dr. K. Sudesh Kumar's office staff for their cooperation and support. I also would like to thank Universiti Sains Malaysia for awarding me with the fellowship at partial of my study period. Last but not least, loving thanks go to my parents, my sister, and my brother who firmly stood by my side and supported me by their encouragements and patience during my PhD study.

TABLE OF CONTENTS

ACKNOWLEDGEMENT	ii
TABLE OF CONTENTS	iii
LIST OF TABLES	ix
LIST OF FIGURES	xii
LIST OF SYMBOLS	xv
LIST OF ABBREVIATIONS	xvi
ABSTRAK	xix
ABSTRACT	xxi
CHAPTER 1 INTRODUCTION	1
1.1 Objective of study	3
CHAPTER 2 LITERATURE REVIEW	5
2.1 Biodegradable and Bio-based polymer	5
2.2 Polyhydroxyalkanoates	6
2.2.1 Background of PHA	6
2.2.2 Structure of PHA granule	8
2.2.3 Properties of PHA.....	11
2.2.4 Types and properties of PHA	13
2.3 Poly(3-hydroxybutyrate) [P(3HB)].....	14
2.4 Poly(3-hydroxybutyrate- <i>co</i> -3-hydroxyhexanoate) [P(3HB- <i>co</i> -3HHx)]	16
2.5 PHA-producing bacteria.....	16
2.6 <i>Cupriavidus necator</i> and its ability to utilize various carbon sources	17
2.7 Glucose as carbon source for PHA biosynthesis.....	18
2.8 NSDG and NSDGΔB1 mutant strains and glucose pathway for P(3HB) and P(3HB- <i>co</i> -3HHx) production.....	19
2.9 Central Composite Design (CCD) and Response Surface Methodology (RSM).....	24

2.10	Fermentation strategies	25
2.11	Cyclic Fed-Batch Fermentation (CFBF).....	26
CHAPTER 3 MATERIALS AND METHODS.....		29
3.1	General methods.....	29
3.1.1	Weighing	29
3.1.2	Measurement of Optical Density (OD)	29
3.1.3	pH measurement.....	29
3.1.4	Sterilization.....	30
3.1.5	Culture incubation	30
3.1.6	Freeze drying	30
3.2	Microorganisms	30
3.2.1	Bacterial strains	30
3.2.2	Maintenance of the pure cultures.....	31
3.3	Culture medium.....	31
3.3.1	Nutrient Rich (NR) medium.....	31
3.3.2	Mineral Salts Medium (MSM).....	32
3.4	Biosynthesis of PHA.....	33
3.4.1	Growth profile for <i>C. necator</i> NSDG-GG and <i>C. necator</i> NSDG-GG Δ B1/pBPP-ccr _{Me} J _{Ac} -emd mutant strains.....	33
3.4.2	Carbon source	33
3.4.3	The effect of different glucose concentration on PHA production by <i>C. necator</i> NSDG-GG and <i>C. necator</i> NSDG-GG Δ B1/pBPP- ccr _{Me} J _{Ac} -emd mutants	34
3.4.4	The effect of different nitrogen sources on PHA production by <i>C.</i> <i>necator</i> NSDG-GG and <i>C. necator</i> NSDG-GG Δ B1/pBPP-ccr _{Me} J _{Ac} - emd mutants.....	34
3.4.5	The effect of different urea concentration on PHA production by <i>C.</i> <i>necator</i> NSDG-GG and <i>C. necator</i> NSDG-GG Δ B1/pBPP-ccr _{Me} J _{Ac} - emd mutants.....	35
3.4.6	One-stage shake flask fermentation for PHA biosynthesis	35

3.5	Analytical procedures.....	35
3.5.1	Determination of residual glucose by High Performance Liquid Chromatography (HPLC)	35
3.5.1(a)	Sample preparation.....	35
3.5.1(b)	HPLC analysis	36
3.5.2	Measurement of Cell Dry Weight (CDW)	37
3.5.3	Gas Chromatography (GC) analysis of P(3HB) and P(3HB- <i>co</i> -3HHx) contents and compositions.....	37
3.5.3(a)	Preparation of methanolysis solution	37
3.5.3(b)	Preparation of Caprylate Methyl Ester (CME)	37
3.5.3(c)	Preparation of sample for Gas Chromatography (GC) analysis.....	38
3.5.3(d)	Gas Chromatography (GC)	38
3.5.3(e)	Determination of P(3HB) and P(3HB- <i>co</i> -3HHx) contents .	39
3.5.4	Central Composite Design (CCD).....	40
3.5.4(a)	Statistical modeling.....	41
3.5.5	Experimental design for the batch and the Cyclic Fed-Batch Fermentation (CFBF) mode.....	43
3.5.5(a)	The seed culture preparation for batch and fed-batch fermentation	43
3.5.5(b)	The bioreactor medium for batch mode.....	44
3.5.5(c)	The bioreactor operation condition	44
3.5.5(d)	Statistical modeling for the batch and the Cyclic Fed-Batch Fermentation (CFBF) mode	46
3.5.5(e)	The bioreactor operation condition for the Cyclic Fed-Batch Fermentation (CFBF) mode.....	46
3.5.5(f)	Calculations of kinetic parameters in batch and fed-batch fermentation	49
3.6	Polymer characterization.....	53
3.6.1	Polymer extraction.....	53
3.6.2	Gel Permeation Chromatography (GPC).....	54

3.6.3	Nuclear Magnetic Resonance (NMR) spectrometry	54
3.6.4	Fourier Transform Infrared (FT-IR) spectroscopy	54
3.6.5	Differential Scanning Calorimetry (DSC).....	55
3.6.6	Thermogravimetric Analysis (TGA)	55
3.6.7	Rheological analysis	56
3.7	Qualitative analysis	56
3.7.1	Phase contrast imaging	56
3.7.2	Observation of PHA inclusions through fluorescence microscope..	56
	3.7.2(a) Preparation of Nile Blue A and acetic acid.....	56
	3.7.2(b) Slide sample preparation for Nile Blue A staining technique	57
3.7.3	Transmission Electron Microscopy (TEM).....	57
	3.7.3(a) Bacterial sample preparation.....	57
	3.7.3(b) Sectioning of TEM sample	59
3.7.4	Statistical analyses	60
CHAPTER 4 RESULTS AND DISCUSSION.....		61
4.1	Growth profile of <i>C. necator</i> NSDG-GG and <i>C. necator</i> NSDG-GGΔB1/pBPP-ccr _{Me} J _{Ac} -emd mutants	61
4.2	Determination of carbon and nitrogen sources and concentrations for PHA biosynthesis by using OFAT	62
4.2.1	The effect of different glucose concentration on PHA production by <i>C. necator</i> NSDG-GG and <i>C. necator</i> NSDG-GGΔB1/pBPP- ccr _{Me} J _{Ac} -emd mutants	62
4.2.2	The effect of different nitrogen sources on PHA production by <i>C.</i> <i>necator</i> NSDG-GG and <i>C. necator</i> NSDG-GGΔB1/pBPP-ccr _{Me} J _{Ac} - emd mutants.....	63
4.2.3	The effect of different urea concentration on PHA production by <i>C.</i> <i>necator</i> NSDG-GG and <i>C. necator</i> NSDG-GGΔB1/pBPP-ccr _{Me} J _{Ac} - emd mutants.....	64
4.3	Optimization of P(3HB) biosynthesis by <i>C. necator</i> NSDG-GG using Central Composite Design (CCD)	66
4.3.1	The effect on biomass production	67

4.3.2	The effect on P(3HB) content.....	70
4.3.3	The effect on P(3HB) concentration.....	74
4.3.4	Validation of the regression model and assay reproducibility studies	77
4.4	Optimization of P(3HB- <i>co</i> -3HHx) biosynthesis by <i>C. necator</i> NSDG-GGΔB1/pBPP- <i>ccr</i> _{Me} J _{Ac} -emd using Central Composite Design (CCD)	79
4.4.1	The effect on biomass production	80
4.4.2	The effect on P(3HB- <i>co</i> -3HHx) content and concentration.....	84
4.4.3	Validation of the regression model and assay reproducibility studies	90
4.5	Batch fermentation mode of P(3HB) and P(3HB- <i>co</i> -3HHx) production in STBR using <i>C. necator</i> NSDG-GG and <i>C. necator</i> NSDG-GGΔB1/pBPP- <i>ccr</i> _{Me} J _{Ac} -emd mutants.....	91
4.5.1	Batch fermentation mode of P(3HB) production in STBR by <i>C. necator</i> NSDG-GG mutant	92
4.5.2	Batch fermentation mode of P(3HB- <i>co</i> -3HHx) production in STBR by <i>C. necator</i> NSDG-GGΔB1/pBPP- <i>ccr</i> _{Me} J _{Ac} -emd mutant.....	93
4.6	Cyclic Fed-Batch Fermentation (CFBF).....	95
4.6.1	Repeated Fed-Batch modes (RFB-I, RFB-II) for the production of P(3HB) and P(3HB- <i>co</i> -3HHx) using <i>C. necator</i> NSDG-GG and <i>C. necator</i> NSDG-GGΔB1/pBPP- <i>ccr</i> _{Me} J _{Ac} -emd mutants	95
4.6.1(a)	Repeated fed-batch cycles of urea (RFB-I), and glucose (RFB-II) in decrement and increment mode at 24 h using <i>C. necator</i> NSDG-GG to produce P(3HB).....	96
4.6.1(b)	Repeated fed-batch cycles of urea (RFB-I), and glucose (RFB-II) in decrement and increment mode at 66 h using <i>C. necator</i> NSDG-GG to produce P(3HB).....	101
4.6.1(c)	Repeated fed-batch cycles of urea (RFB-I) and glucose in constant mode at 42 h using <i>C. necator</i> NSDG-GG to produce P(3HB)	103
4.6.1(d)	Pareto chart analysis	107
4.6.1(e)	The model-based fed-batch of urea and glucose using <i>C. necator</i> NSDG-GG to produce P(3HB).....	108
4.6.1(f)	Repeated Fed-Batch cycles of urea (RFB-I), and glucose (RFB-II) in decrement and increment mode at 24 h using <i>C.</i>	

	<i>necator</i> NSDG-GGΔB1/pBPP- <i>ccr</i> _{Me} J _{Ac} -emd mutant to produce P(3HB- <i>co</i> -3HHx).....	112
4.6.1(g)	Repeated Fed-Batch cycles of urea (RFB-I), and glucose (RFB-II) in decrement and increment mode at 66 h using <i>C. necator</i> NSDG-GGΔB1/pBPP- <i>ccr</i> _{Me} J _{Ac} -emd mutant to produce P(3HB- <i>co</i> -3HHx)	115
4.6.1(h)	Repeated Fed-Batch cycles of urea (RFB-I), and glucose in constant mode at 42 h using <i>C. necator</i> NSDG-GGΔB1/pBPP- <i>ccr</i> _{Me} J _{Ac} -emd mutant to produce P(3HB- <i>co</i> -3HHx).....	116
4.6.1(i)	Pareto chart analysis	121
4.6.1(j)	The model-based fed-batch of urea and glucose using <i>C. necator</i> NSDG-GGΔB1/pBPP- <i>ccr</i> _{Me} J _{Ac} -emd mutant to produce (3HB- <i>co</i> -3HHx).....	123
4.6.2	The summary effect of various cultivation systems on the maximum biomass, P(3HB) and P(3HB- <i>co</i> -3HHx) concentration using <i>C. necator</i> NSDG-GG and <i>C. necator</i> NSDG-GGΔB1/pBPP- <i>ccr</i> _{Me} J _{Ac} -emd mutants.....	126
4.7	Polymer characterization.....	128
4.7.1	Gel Permeation Chromatography (GPC).....	128
4.7.2	Differential Scanning Calorimetry (DSC).....	130
4.7.3	Thermogravimetric Analysis (TGA)	131
4.7.4	Nuclear Magnetic Resonance (NMR) spectrometry	133
4.7.5	Fourier Transform Infrared (FT-IR) spectroscopy	135
4.7.6	Rheological analysis	136
4.8	Observation of cells by microscopy.....	137
4.8.1	Observation of PHA through Fluorescence Microscope and Transmission Electron Microscopy (TEM).....	137
	CHAPTER 5 CONCLUSION	140
	REFERENCES.....	142
	APPENDICES	
	LIST OF PUBLICATIONS	

LIST OF TABLES

		Page
Table 2.1	Properties of common types of PHAs synthesized by bacteria	14
Table 2.2	General comparison of scl- and mcl-PHA.....	15
Table 3.1	The composition of NR medium.....	31
Table 3.2	The composition of MSM medium.....	32
Table 3.3	The composition of trace elements solution	33
Table 3.4	Test variables and levels of Central Composite Design (CCD) to produce P(3HB) by <i>C. necator</i> NSDG-GG mutant.....	41
Table 3.5	Test variables and levels of Central Composite Design (CCD) to produce P(3HB-co-3HHx) using <i>C. necator</i> NSDG-GGΔB1/pBPP-ccr _{Me} J _{Ac} -emd mutant	41
Table 3.6	Factors and coded values of Fractional Factorial Design (2 ³⁻¹ FFD) to produce (P(3HB) and P(3HB-co-3HHx)).....	43
Table 3.7	The method of repeated fed-batch mode based on the 2 ³⁻¹ FFD to produce (P(3HB)).....	47
Table 3.8	The method of repeated fed-batch mode based on the 2 ³⁻¹ FFD to produce P(3HB-co-3HHx).....	48
Table 4.1	The effect of types and concentrations of nitrogen sources for P(3HB) and P(3HB-co-3HHx) biosynthesis by <i>C. necator</i> NSDG-GG and <i>C. necator</i> NSDG-GGΔB1/pBPP-ccr _{Me} J _{Ac} -emd in MSM broth with 25 g/L ad 20 g/L glucose, respectively	64
Table 4.2	Central Composite Design (CCD) and experimental values for biomass (g/L), P(3HB) content (wt%), and P(3HB) concentration (g/L) produced by <i>C. necator</i> NSDG-GG in batch shake flask fermentation at 30 °C for 48 h.....	67
Table 4.3	Analysis of variance for the second-order polynomial model of biomass synthesis by <i>C. necator</i> NSDG-GG mutant in batch fermentation at 30 °C for 48 h.....	69
Table 4.4	Analysis of variance for the second-order polynomial model of P(3HB) content produced by <i>C. necator</i> NSDG-GG in batch fermentation at 30 °C for 48 h.....	73

Table 4.5	Analysis of variance for the second-order polynomial model of P(3HB) concentration produced by <i>C. necator</i> NSDG-GG in batch fermentation at 30 °C for 48 h.....	76
Table 4.6	Optimized cultivation conditions, predicted, and experimental values for biomass, P(3HB) content, and P(3HB) concentration production using <i>C. necator</i> NSDG-GG.....	78
Table 4.7	Central Composite Design (CCD) and experimental values for biomass (g/L), P(3HB- <i>co</i> -3HHx) content (wt%), and P(3HB- <i>co</i> -3HHx) concentration produced by <i>C. necator</i> NSDG-GG Δ B1/pBPP- <i>ccr</i> _{Me} J _{Ac} -emd mutant in batch shake flask fermentation at 30 °C for 48 h.....	80
Table 4.8	Analysis of variance for the second-order polynomial model of biomass synthesis by <i>C. necator</i> NSDG-GG Δ B1/pBPP- <i>ccr</i> _{Me} J _{Ac} -emd in batch fermentation at 30 °C for 48 h	83
Table 4.9	Analysis of variance for the second-order polynomial model of P(3HB- <i>co</i> -3HHx) content produced by <i>C. necator</i> NSDG-GG Δ B1/pBPP- <i>ccr</i> _{Me} J _{Ac} -emd in batch fermentation at 30°C for 48 h	84
Table 4.10	Analysis of variance for the second-order polynomial model of P(3HB- <i>co</i> -3HHx) concentration produced by <i>C. necator</i> NSDG-GG Δ B1/pBPP- <i>ccr</i> _{Me} J _{Ac} -emd in batch fermentation at 30 °C for 48 h	89
Table 4.11	Optimized cultivation conditions, predicted, and experimental values for biomass, P(3HB- <i>co</i> -3HHx) content, and P(3HB- <i>co</i> -3HHx) concentration production using <i>C. necator</i> NSDG-GG Δ B1/pBPP- <i>ccr</i> _{Me} J _{Ac} -emd.....	91
Table 4.12	Kinetics parameters resulting from the fed-batch runs of fractional factorial design (2^{3-1} FFD) to produce P(3HB) by <i>C. necator</i> NSDG-GG mutant.....	105
Table 4.13	Experimental design, and results of fractional factorial design (2^{3-1} FFD).....	106
Table 4.14	Regression results of fractional factorial design (2^{3-1} FFD).....	106
Table 4.15	Regression model summary for the total biomass (X_T) and PHA (P_T)	107
Table 4.16	The results for the final run repeated fed-batch fermentation	111

Table 4.17	Kinetics parameters resulting from the fed-batch runs of fractional factorial design (2^{3-1} FFD) to produce P(3HB- <i>co</i> -3HHx) by <i>C. necator</i> NSDG-GG Δ B1/pBPP- <i>ccr</i> _{MeJ_{Ac}-emd mutant.....}	119
Table 4.18	Experimental design and results of fractional factorial design (2^{3-1} FFD).....	120
Table 4.19	Regression results of fractional factorial design (2^{3-1} FFD).....	120
Table 4.20	Regression model summary for the total biomass (X_T) and PHA (P_T).....	121
Table 4.21	The results for the final run repeated fed-batch fermentation.....	125
Table 4.22	The summary effect of various cultivation systems on the maximum biomass and P(3HB) concentration using <i>C. necator</i> NSDG-GG mutant.....	127
Table 4.23	The summary effect of various cultivation systems on the maximum biomass, (3HB- <i>co</i> -3HHx) concentration, and 3HHx content using <i>C. necator</i> NSDG-GG Δ B1/pBPP- <i>ccr</i> _{MeJ_{Ac}-emd mutant.....}	128
Table 4.24	Gel Permeation Chromatography (GPC) analysis for P(3HB) and P(3HB- <i>co</i> -3HHx) by <i>C. necator</i> NSDG-GG and <i>C. necator</i> NSDG-GG Δ B1/pBPP- <i>ccr</i> _{MeJ_{Ac}-emd mutants.....}	130
Table 4.25	Thermal characterization of P(3HB) and P(3HB- <i>co</i> -3HHx) produced by <i>C. necator</i> NSDG-GG and NSDG-GG Δ B1/pBPP- <i>ccr</i> _{MeJ_{Ac}-emd mutants from glucose.....}	131

LIST OF FIGURES

		Page
Figure 2.1	The processes to produce bio-based polymers.....	6
Figure 2.2	Structure of PHA.....	7
Figure 2.3	Model of an <i>in vivo</i> P(3HB) granule in <i>C. necator</i> H16.....	9
Figure 2.4	Classification of PHA synthases.....	10
Figure 2.5	PHA biosynthetic pathways in bacteria.....	12
Figure 3.1	Schematic representation of the fill-and-draw fed-batch mode of fermentation system.....	45
Figure 3.2	Scheme of sampling and repeated culture volume replacement (5%, 7.5%, and 10%) in a Fill-And-Draw (F/D) cyclic fed-batch modes of glucose (RFB-II).....	49
Figure 4.1	Growth profiles of <i>C. necator</i> NSDG-GG and <i>C. necator</i> NSDG-GG Δ B1/pBPP-ccr _{Me} J _{Ac} -emd mutants in NR broth inoculated at 30 °C.....	61
Figure 4.2	The effect of glucose concentration on biomass and PHA biosynthesis.....	63
Figure 4.3	The effect of urea concentration on biomass and PHA biosynthesis.....	65
Figure 4.4	3D surface showing the interactive effect of input-independent variables on biomass production after 48 h of cultivation.....	70
Figure 4.5	3D surface showing the interactive effect of input-independent variables on P(3HB) content after 48 h of cultivation.....	74
Figure 4.6	3D surface showing the interactive effect of input-independent variables on P(3HB) concentration.....	76
Figure 4.7	3D surface showing the interactive effect of input-independent variables on biomass production after 48 h of cultivation.....	83
Figure 4.8	3D surface showing the interactive effect of input-independent variables on P(3HB-co-3HHx) content after 48 h of cultivation.....	85

Figure 4.9	3D surface showing the interactive effect of input-independent variables on P(3HB-co-3HHx) concentration after 48 h of cultivation.....	89
Figure 4.10	Time course profile of batch fermentation parameters in STBR by <i>C. necator</i> NSDG-GG mutant.....	93
Figure 4.11	Time course profile of batch fermentation parameters in STBR by <i>C. necator</i> NSDG-GGΔB1/pBPP-ccr _{Me} J _{Ac} -emd mutant.....	95
Figure 4.12	Time course profile of fermentation parameters resulting from repeated fed-batch cycles of urea and glucose starting at 24 h by <i>C. necator</i> NSDG-GG mutant.....	100
Figure 4.13	Time course profile of fermentation parameters resulting from repeated fed-batch cycles of urea and glucose starting at 66 h by <i>C. necator</i> NSDG-GG mutant.....	102
Figure 4.14	Time course profile of fermentation parameters resulting from constant† [glucose] repeated fed-batch cycles (RFB-II) starting at 42 h by <i>C. necator</i> NSDG-GG mutant.....	104
Figure 4.15	The effect of glucose mode in repeated fed-batch cycle regime on biomass (X_t and X_r) and PHA production by <i>C. necator</i> NSDG-GG mutant	107
Figure 4.16	Pareto chart analysis of the effect of terms (X_1 , X_2 , and X_3) on the total biomass (X_T), residual biomass (X_R), and PHA (P_T) concentration by <i>C. necator</i> NSDG-GG mutant	108
Figure 4.17	The schematic (I) and graphical (II) representation of the volume replacement (7.5%) in a fill-and-draw (F/D) cyclic fed-batch mode of urea and/or glucose by <i>C. necator</i> NSDG-GG mutant	110
Figure 4.18	Time course profile of fermentation parameters resulting from the repeated fed-batch cycles of urea and glucose by <i>C. necator</i> NSDG-GG mutant.....	112
Figure 4.19	Time course profile of fermentation parameters resulting from repeated fed-batch cycles of urea and glucose starting at 24 h by <i>C. necator</i> NSDG-GGΔB1/pBPP-ccr _{Me} J _{Ac} -emd mutant	114
Figure 4.20	Time course profile of fermentation parameters resulting from repeated fed-batch cycles of urea and glucose starting at 66 h by <i>C. necator</i> NSDG-GGΔB1/pBPP-ccr _{Me} J _{Ac} -emd mutant	116
Figure 4.21	Time course profile of fermentation parameters resulting from constant† [glucose] repeated fed-batch cycles (RFB-	

	II) starting at 42 h by <i>C. necator</i> NSDG-GGΔB1/pBPP- ccr _{Me} J _{Ac} -emd mutant	118
Figure 4.22	The effect of glucose mode in repeated fed-batch cycle regime on biomass (X_t and X_r) and PHA production by <i>C. necator</i> NSDG-GGΔB1/pBPP-ccr _{Me} J _{Ac} -emd mutant	121
Figure 4.23	Pareto chart analysis of the effect of terms (X_1 , X_2 , and X_3) on the total biomass (X_T), residual biomass (X_R), and PHA (P_T) concentration by <i>C. necator</i> NSDG-GGΔB1/pBPP-ccr _{Me} J _{Ac} -emd mutant	122
Figure 4.24	The schematic (I) and graphical (II) representation of the volume replacement (8.2%; 88%; 9.4%) in a fill-and-draw (F/D) cyclic fed-batch mode of urea and/or glucose by <i>C. necator</i> NSDG-GGΔB1/pBPP-ccr _{Me} J _{Ac} -emd mutant.....	124
Figure 4.25	Time course profile of fermentation parameters resulting from the repeated fed-batch cycles of urea and glucose by <i>C. necator</i> NSDG-GGΔB1/pBPP-ccr _{Me} J _{Ac} -emd mutant.....	126
Figure 4.26	TGA thermogram of P(3HB) and P(3HB-co-3HHx).....	133
Figure 4.27	500 MHz ¹ H NMR spectrum confirming the presence of 3HB unit in P(3HB) produced by <i>C. necator</i> NSDG-GG mutant from glucose as carbon source	134
Figure 4.28	500 MHz ¹ H NMR spectrum confirming the presence of 3HHx unit in P(3HB-co-3HHx) produced by <i>C. necator</i> NSDG-GGΔB1/pBPP-ccr _{Me} J _{Ac} -emd mutant from glucose as carbon source	135
Figure 4.29	FTIR spectra of P(3HB) using <i>C. necator</i> NSDG-GG and FTIR spectra of P(3HB-co-3HHx) using <i>C. necator</i> NSDG-GGΔB1/pBPP-ccr _{Me} J _{Ac} -emd grown on glucose as carbon source	136
Figure 4.30	The dynamic viscosity as a function of time at 200 °C for P(3HB) produced by <i>C. necator</i> NSDG-GG and <i>C. necator</i> H16, and P(3HB-co-3HHx) produced by <i>C. necator</i> NSDG-GGΔB1/pBPP-ccr _{Me} J _{Ac} -emd	137
Figure 4.31	Fluorescence microscopic of P(3HB) granule in <i>C. necator</i> NSDG-GG cells and P(3HB-co-3HHx) granule in <i>C. necator</i> NSDG-GGΔB1/pBPP-ccr _{Me} J _{Ac} -emd cells	139
Figure 4.32	TEM micrograph of P(3HB) granule in <i>C. necator</i> NSDG-GG cells and P(3HB-co-3HHx) granule in <i>C. necator</i> NSDG-GGΔB1/pBPP-ccr _{Me} J _{Ac} -emd cells	139

LIST OF SYMBOLS

\sim	Approximately
β	Beta
$^{\circ}\text{C}$	Degree Celsius
ΔH_m	Enthalpy of fusion
$>$	Greater-than
$<$	Less-than
\pm	Plus-minus
\times	Times

LIST OF ABBREVIATIONS

3HB	3-hydroxybutyrate
3HHx	3-hydroxyhexanoate
C	Carbon atom
¹³ C	Carbon-13
CCD	Central Composite Design
C/N	Carbon to Nitrogen
CDW	Cell Dry Weight
CFBF	Cyclic Fed-Batch Fermentation
CH	Methine group
CH ₂	Methylene group
CH ₃	Methyl group
CME	Caprylic Methyl Ester
CoA	Coenzyme-A
DO	Dissolved Oxygen
F/D	Fill-and-Draw
FT-IR	Fourier Transform Infrared spectrometry
GC	Gas Chromatography
GPC	Gel Permeation Chromatography
¹ H	Proton
HCDC	High Cell Density Cultivation
h	Hour
HA	Hydroxyalkanoic Acid
kDa	Kilodalton
mcl-	Medium chain-length
min	Minute

MSM	Mineral Salts Medium
M	Molarity
mol%	Mol percent
M_n	Number average molecular weight
M_w	Weight average molecular weight
M_w/M_n	Polydispersity index
N	Normality
NMR	Nuclear Magnetic Resonance
NR	Nutrient rich
OD	Optical Density
OFAT	One-factor-at-a-time
P(3HB- <i>co</i> -3HHx)	Poly(3-hydroxybutyrate- <i>co</i> -3-hydroxyhexanoate)
PBS	Polybutylene succinate
PE	Polyethylene
PHA	Polyhydroxyalkanoate
PLA	Polylactic acid
PPP	Poly(p-phenylene)
PTT	Polytrimethylene terephthalate
RG	Residual Glucose
RFB	Repeated Fed-Batch
RFB-I	Repeated Fed-Batch-I
RFB-II	Repeated Fed-Batch-II
rpm	Revolutions Per Minute
s	Second
scl-	Short chain-length
STBR	Stirred-tank bioreactor
TEM	Transmission Electron Microscope

T_g	Glass transition temperature
T_m	Melting temperature
v/v	Volume per volume
wt%	Weight percent
w/v	Weight per volume
w/w	Weight per weight

**PENGHASILAN POLIHIDROKSIALKANOAT DARIPADA GLUKOSA
OLEH MUTAN *Cupriavidus necator* MELALUI STRATEGI FERMENTASI
INOVATIF**

ABSTRAK

Polihidroksialkanoat (PHA) disintesis secara intraselular oleh pelbagai mikroorganisma dan mempunyai potensi sebagai polimer terbiodegradasi. Disebabkan oleh produktiviti dan hasil yang sedikit, hanya beberapa mikroorganisma dikulturkan pada skala industri untuk menghasilkan PHA yang menggunakan sumber karbon semulajadi yang banyak. *Cupriavidus necator* H16 jenis liar ialah strain yang boleh menggunakan beberapa jenis gula ringkas dan minyak tetapi tidak boleh menggunakan glukosa. Mutan *C. necator* NSDG-GG dan *C. necator* NSDG-GG Δ B1/pBPP-ccr_{Me}J_{Ac}-emd ialah strain baharu yang digunakan untuk menghasilkan PHA daripada glukosa. Kajian ini bertujuan untuk mengoptimumkan kondisi kultur bagi menghasilkan polimer poli(3-hidroksibutirat) [P(3HB)] dan poli(3-hidroksibutirat-*ko*-3-hidroksiheksanoat) [P(3HB-*ko*-3HHx)] dengan menggunakan jenis mutan yang baharu. Pada awal eksperimen, julat kepekatan nutrient (urea dan glukosa) yang bersesuaian ditentukan untuk mendapatkan biomas dan PHA yang tinggi dengan menggunakan pendekatan satu-faktor-pada-satu-masa (OFAT). Kemudian, metodologi respon permukaan (RSM) telah diaplikasikan dalam pengoptimuman beberapa kunci parameter pada waktu yang sama bagi mencapai kondisi optimum untuk meningkatkan sel biomas dan penghasilan PHA dalam satu sistem pelbagai-pembolehubah. Komposisi optimum media yang meningkatkan

biomas dan penghasilan PHA telah digunakan dalam pengkulturan mod suapan kelompok “fed-batch” untuk meningkatkan biomas sel dan penghasilan PHA menggunakan bioreaktor 5 L. Seterusnya, strategi isi-dan-buang (F/D) suapan kelompok dilaksanakan untuk memahami kunci parameter yang memberi impak kepada jumlah sel densiti dan kepekatan PHA dalam peningkatan dan penurunan mod suapan kelompok. Strategi mendedahkan bahawa kitaran suapan kelompok “fed-batch di dalam sebuah bioreaktor tangki teraduk (STBR) secara signifikannya meningkatkan biomas kepada 84.80 g/L (7×) dan kepekatan PHA kepada 62.00 g/L (5×) berbanding pengkulturan berperingkat di dalam sistem goncangan kelalang *C. necator* NSDG-GG. Tambahan itu, berbanding RSM, strategi kitaran suapan kelompok “fed-batch” di dalam STBR dengan banyaknya meningkatkan biomas, kepekatan PHA, pecahan 3HHx masing-masingnya dalam anggaran 6× (45.34 g/L), 7× (29.47 g/L), dan 4× (18 mol%), berbanding RSM oleh *C. necator* NSDG-GGΔB1/pBPP-ccr_{Me}J_{Ac}-emd. Akhirnya, homo-polimer P(3HB) dan P(3HB-ko-3HHx) ko-polimer yang terhasil dicirikan dan didapati mempunyai sifat yang lebih baik daripada yang berasal daripada jenis liar. Penemuan daripada kajian ini mencadangkan bahawa kedua-dua strain baharu *C. necator* NSDG-GG dan *C. necator* NSDG-GGΔB1/pBPP-ccr_{Me}J_{Ac}-emd yang dijanakan mempunyai potensi untuk menghasilkan PHA daripada glukosa.

POLYHYDROXYALKANOATES PRODUCTION BY *Cupriavidus necator*
MUTANTS FROM GLUCOSE BY INNOVATIVE FERMENTATION
STRATEGIES

ABSTRACT

Polyhydroxyalkanoate (PHA) is synthesized intracellularly by many microorganisms and has potential as a biodegradable polymer. Due to the low productivity and yield, only few microorganisms have been cultivated at industrial scale to produce the PHA using natural and abundant carbon source. *Cupriavidus necator* wild strain H16 can assimilate some simple sugars and oils but does not utilize glucose. *C. necator* NSDG-GG and *C. necator* NSDG-GGΔB1/pBPP-ccr_{Me}J_{Ac}-emd mutants are new strains developed to produce PHA from glucose. The purpose of this study was to optimize the culture conditions to produce poly(3-hydroxybutyrate) [P(3HB)] and poly(3-hydroxybutyrate-co-3-hydroxyhexanoate) [P(3HB-co-3HHx)] polymers by using these new mutants. Initially, appropriate ranges of nutrients concentration (urea and glucose) were determined to obtain the highest biomass and PHA by using the one-factor-at-a-time (OFAT) approach. Then, a response surface methodology (RSM) was applied to optimize the key variables at-a-time to attain the optimal condition of biomass and PHA production in a multivariable system. The optimized medium compositions which improved the biomass and PHA production, were used to design fed-batch cultivation modes to scale-up the biomass and PHA production in a 5 L bioreactor. Subsequently, a fill-and-draw (F/D) fed-batch strategy was employed to understand the key parameters that impacted the total cell densities and PHA concentration in the increment and decrement fed-batch modes. The strategy revealed that the fed-batch cycles in the

stirred-tank bioreactor (STBR) system significantly increased the biomass to 84.80 g/L (7×) and PHA concentration to 62.00 g/L (5×) as compared to that of batch cultivation in shake flask system (RSM) by *C. necator* NSDG-GG. Furthermore, compared to RSM, the strategy of fed-batch cycles in STBR greatly improved the biomass, PHA concentration, and 3HHx fraction by approximately 6× (45.34 g/L), 7× (29.47 g/L), and 4× (18 mol%), respectively, by *C. necator* NSDG-GG Δ B1/pBPP-ccr_{Me}J_{Ac}-emd. Finally, the P(3HB) homopolymer and P(3HB-co-3HHx) copolymers were characterized and were found to have better properties than those from the wild-type. The findings of this study suggest that the two newly engineered strains of *C. necator* NSDG-GG and *C. necator* NSDG-GG Δ B1/pBPP-ccr_{Me}J_{Ac}-emd have potential for production of PHA from glucose.

CHAPTER 1

INTRODUCTION

In the various industries, petrochemical plastic has become one of the most intensively used materials all over the world, but their disposal still poses a serious problem to the environment because of their non-degradable characteristics. In addition, recently the serious issue of microplastics in the ocean and in our environment including food have been reported (Chatterjee & Sharma, 2019). For this reason, researchers are developing biodegradable plastics such as polyhydroxyalkanoates (PHAs) (Tan et al., 2014).

PHA has thermo-mechanical properties similar to petrochemical polymers such as polypropylene (PP) and polyethylene (PE) with a biodegradable characteristic in the environment (Lee, 1996; Sudesh, 2013). Nevertheless, the production of PHA from renewable resources and their complete biodegradability give these biopolymers distinctive advantages (Braunegg et al., 1978; Byrom, 1987). Thus, it makes them more convenient for environmentally friendly products with numerous applications in industries. Therefore, the PHA biopolymers are considered the future material to replace the non-biodegradable petro-based plastic (Steinbüchel & Fächtenbusch, 1998).

Generally, PHA is a variety of biodegradable polymer that is synthesized intracellularly by many genera of bacteria (Narayanan & Ramana 2012). But due to the low productivity and yield, only a few microorganisms have been cultivated at industrial scale to produce the PHA (García et al., 2014; Ienczak et al., 2013). *Cupriavidus necator* is one strain that have been investigated to produce PHA with

some advantages as to obtain high cell density culture (HCDC) for PHA bioprocess production (Choi & Lee, 1999).

The raw materials for PHA production vary from sugars to plant oils. In this context, *C. necator* and some of its genetically modified organisms (GMO) and many other PHA producing microorganisms do not have enzymes to utilize complex sugars from agro-wastes. This has resulted in the utilization of only simple types of sugar for PHA production (Jiang et al., 2016). Moreover, *C. necator* wild strain H16 could assimilate some simple sugars such as fructose and gluconate but does not utilize glucose. So far, a few glucose-utilizing mutants of *C. necator* have been isolated by UV and spontaneous mutagenesis (Raberg et al. 2012) and constructed by targeted genetic engineering (Poirier et al. 1992). The *C. necator* NSDG-GG and *C. necator* NSDG-GG Δ B1/pBPP-ccI_{Me}J_{Ac}-emd mutants are as modified strains to accumulate poly(3-hydroxybutyrate) [P(3HB)] and poly(3-hydroxybutyrate-co-3-hydroxyhexanoate) [P(3HB-co-3HHx)] from glucose.

One-factor-at-a-time (OFAT) is a suitable method to identify the considerable factors and their useful operational ranges. However, they rarely evaluate the effect of more than a factor at a time and their interactions, which is a weakness once the interactions of factors are significant. Generally, the feature of the bioprocesses is characterized by the interactions among the level of their input factors (Surwase et al., 2013; Wang & Wan, 2009). Hence, in the quantitative optimization of bioprocess, a robust design of experiment must be applied by which the input parameter levels and their interactions can be analyzed. To this point, the central composite design (CCD) has been determined as the most popular design for RSM to fit models. The present study has a unique feature of applying statistical optimization

of P(3HB) and P(3HB-co-3HHx) by *C. necator* NSDG-GG and *C. necator* NSDG-GG Δ B1/pBPP-ccr_{Me}J_{Ac}-emd mutants from glucose.

PHA production has some limitations as well. Several fed-batch fermentation processes have been developed and reported to produce PHA effectively (Kessler et al., 2001; Lee et al., 2000) because of achieving a high cell concentration that allows increased productivity but the yield of PHA are complicated (Solaiman et al., 2006; Yamanè & Shimizu, 1984). Consequently, in the literature, various strategies of fed-batch modes have been designed (Ienczak et al., 2013; Lee & Kim, 2001; Mears et al., 2017). Therefore, in order to control substrates concentration in fed-batch cycles, a simple empirical control strategy (open loop control) based on increment and decrement repeated fed-batch of glucose was designed and applied in a fill-and-draw mode with *C. necator* NSDG-GG and *C. necator* NSDG-GG Δ B1/pBPP-ccr_{Me}J_{Ac}-emd mutants. The present fed-batch mode study will provide the insight about the physiological stability, volume dynamics effect of medium replacement, and the productivity parameters of the mutants in stirred-tank bioreactor (STBR).

1.1 Objective of study

The main objective of the present study is the evaluation of PHA production including P(3HB) homopolymer and P(3HB-co-3HHx) copolymer by *C. necator* NSDG-GG and *C. necator* NSDG-GG Δ B1/pBPP-ccr_{Me}J_{Ac}-emd mutants from glucose. The study objective consists of the specific aims listed below:

- Specific aim 1: Determination of carbon and nitrogen sources and concentrations for PHA biosynthesis by using one-factor-at-a-time (OFAT)

- Specific aim 2: Statistical modeling optimization applying response surface methodology (RSM)
- Specific aim 3: Statistical optimization using the first order model obtained from fractional factorial design (2^{3-1} FFD) in a fill-and-draw (F/D) fed-batch mode in STBR-system
- Specific aim 4: The characterization of P(3HB) and P(3HB-co-3HHx) polymers

CHAPTER 2

LITERATURE REVIEW

2.1 Biodegradable and Bio-based polymer

Polymers that can be fully degraded in the environment and are not harmful to flora and fauna are commonly termed as biodegradable polymers. Examples of such biobased and natural polymers are polyhydroxyalkanoates (PHA), polylactide (PLA), poly(ϵ -caprolactone) (PCL), poly(p-dioxanone) (PPDO), poly(butylene succinate) (PBS), natural fibres, hydrogels, starch cellulose, chitin, chitosan, and lignin (Akaraonye et al., 2010; Niaounakis, 2014). In general, biopolymers can be classified into 3 main groups: 1) Bio-chemosynthetic polymers, produced by the chemical polymerization of monomers derived from biological processes, for example PLA and PBS, 2) Biosynthetic polymers, produced from microorganisms through biosynthesis, such as PHA, and 3) Modified natural polymers, consisting of starch and cellulose derivatives. These biopolymers possess better properties thus making them much suitable as bio-based polymers (Sudesh & Iwata, 2008).

Bio-based polymers can be either biodegradable (starch and polyhydroxyalkanoates) or non-degradable (biopolyethylene) (Babu et al., 2013). It is well known that not all bio-based polymers are biodegradable such as PLA, polythioesters and cellulose ester derivatives. PLA is not biodegradable, but it can be hydrolysed in water at high temperatures of above 60 °C, whereas the modified natural polymers can only be enzymatically degraded (Sudesh & Iwata, 2008). PLA as distinct from PHA undergoes both hydrolysis and enzymatic reactions. Woolnough et al. (2010) found that PHA has the shortest period of degradation (40-50 days) as compared to other bio-based polymers (Woolnough et al., 2010).

Therefore, PHA with such unique properties has drawn a great deal of attention and interest as a suitable replacement for petrochemical synthetic polymers (Sudesh & Doi, 2000; Sudesh et al., 2000; Tsuge, 2002). Bio-based polymers are divided into three main categories - agro resources, microorganisms and biotechnology approach, respectively (Figure 2.1).

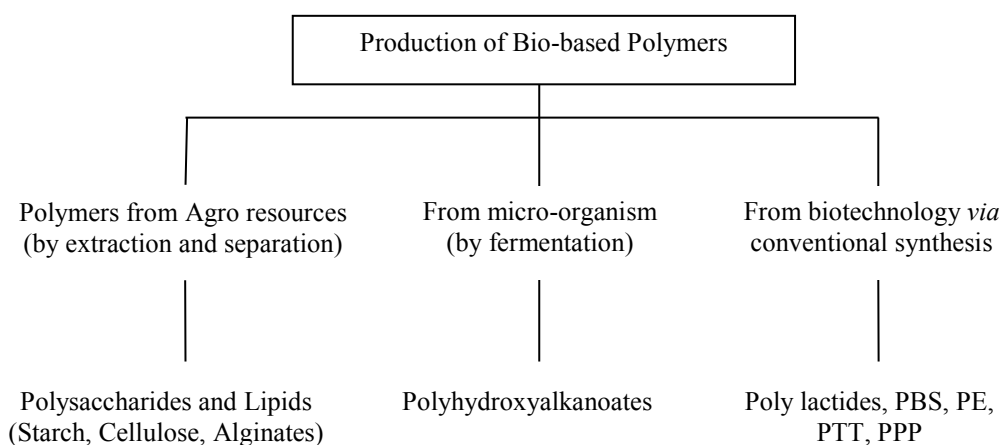


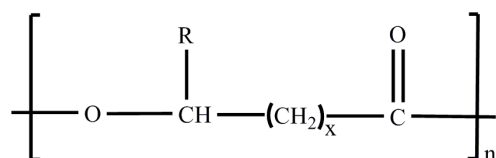
Figure 2.1. The processes to produce bio-based polymers

2.2 Polyhydroxyalkanoates

2.2.1 Background of PHA

Polyhydroxyalkanoates (PHAs), among all bio-based polymers, are the most prominent polymers that have been currently and intensively studied. PHAs are made of 3-hydroxyalkanoic acid (3HA) monomers that are biosynthesized by Gram-positive (Findlay & White, 1983; Williamson & Wilkinson, 1958) and Gram-negative (Forsyth et al., 1958) bacteria and can act as a most ideal form of intracellular carbon and energy storage. PHAs can also be synthesized by archaeobacteria (Kaur et al., 2017). PHA is an ideal storage compound because it is insoluble in the bacterial cytoplasm and therefore produces negligible increase in the osmotic pressure in the cell (Anderson & Dawes, 1990). Moreover, these polymers

can be accumulated to the level as high as 90% of the cell dry weight (Kato et al., 1996; Madison & Huisman, 1999). A subset of PHA, i.e., poly-3-hydroxybutyrate [P(3HB)] was first discovered in *Bacillus megaterium* by Lemoigne in 1926 (Lemoigne, 1926). In 1958, Macrae and Wilkinson successfully proved that the PHAs in bacterial cells were produced during an increase of carbon to nitrogen ratio (Macrae & Wilkinson, 1958). Subsequently, studies uncovered more than 150 monomer constituents of PHA (Steinbüchel, 2001; Steinbüchel & Valentin, 1995; Urtuvia et al., 2014). Apart from P(3HB), other monomers such as 3-hydroxyvalerate (3HV), 3-hydroxyhexanoate (3HHx) and 3-hydroxyheptanoate (3HHp) were also discovered (Wallen & Rohwedder, 1974). In 1983, 3-hydroxyoctanoate (3HO) was identified from *Pseudomonas oleovorans* (De Smet et al., 1983). PHA consists of (*R*)-3-hydroxyalkanoic acids linked by hydroxyl and carboxyl groups of an adjacent monomer. Figure 2.2 shows the chemical structure of PHA.



Number of repeating units, x	Alkyl group, R	Type of monomer
1	hydrogen	3-hydroxypropionate
	methyl	3-hydroxybutyrate
	ethyl	3-hydroxyvalerate
	propyl	3-hydroxyhexanoate
	pentyl	3-hydroxyoctanoate
	nonyl	3-hydroxydodecanoate
2	hydrogen	4-hydroxybutyrate
	methyl	4-hydroxyvalerate
3	hydrogen	5-hydroxyvalerate
	methyl	5-hydroxyhexanoate

Figure 2.2. Structure of PHA
 [Source: (Lee, 1996; Sudesh et al., 2000)]

PHA monomers can appear in diverse forms. This diversity depends on substrate specificity of PHA synthase and carbon sources, which will in turn influence the metabolic pathways of microorganisms (Loo & Sudesh, 2007). PHA synthases are usually highly stereospecific and can only polymerise (*R*) enantiomer of HA monomer (Sudesh et al., 2000). In the process of polymerization, PHA synthase determines the size of monomers. As the molecular weight is dependent on size, PHA synthase influences the final molecular weight of PHA (Loo & Sudesh, 2007).

The grouping shown in Figure 2.2 is based on the substrate specificity of PHA synthases, as it is the key enzyme involved in the biosynthesis of PHA. PHA synthase enzyme that stems from different bacteria can possess different substrate specificities. Most of the PHA synthases can only polymerize either scl monomers or mcl monomers. However, some other PHA synthases have been found to be able to polymerize both the scl and mcl monomers. *Cupriavidus necator*, formerly known as *Alcaligenes eutrophus* or *Wautersia eutropha* can produce scl-PHA that incorporates 3HB, 3HV, and 4HB monomers (Kunioka et al., 1989; Saito et al., 1996). On the other hand, *Pseudomonas oleovorans*, *Pseudomonas putida*, *Aeromonas caviae*, and *Nocardia coralline* can synthesize mcl-PHA consisting of 3HHx, 3HO and 3-hydroxydecanoate (3HD) monomers (De Smet et al., 1983; Lee et al., 2000).

2.2.2 Structure of PHA granule

PHA/P(3HB) granules are supra-molecular complexes in prokaryotes. They are termed as carbonosomes and are composed of P(3HB) polymer core and surrounded by a surface layer of structural and functional proteins. Lately, research have indicated that phospholipids are not found in PHA/P(3HB) granules; they,

however, consists mainly of proteins on the surface layers (Bresan et al., 2016) (Figure 2.3). PHA synthase, intracellular PHA depolymerase, Phasins, PhaR (protein with regulatory function), and other PHA-associated proteins are among the proteins that are bound to PHA granule. Granule-associated proteins are conceived as Phasins (PhaPs) quite similar to oleosins which are proteins found on the surface of oil globules in some plant cells (Steinbüchel et al., 1995). Surprisingly, it was shown that PhaP can form a proteinaceous boundary layer between the hydrophobic polymer and the hydrophilic cytoplasm, and this action determines the surface-to-volume ratio of P(3HB) granules and thus avoids the coalescence of P(3HB) granules *in vivo*. These phasins are found in all the PHA-accumulating bacteria (Wieczorek et al., 1996). In the meantime, the characteristic outcome of PhaP is regulated by repressor PhaR.

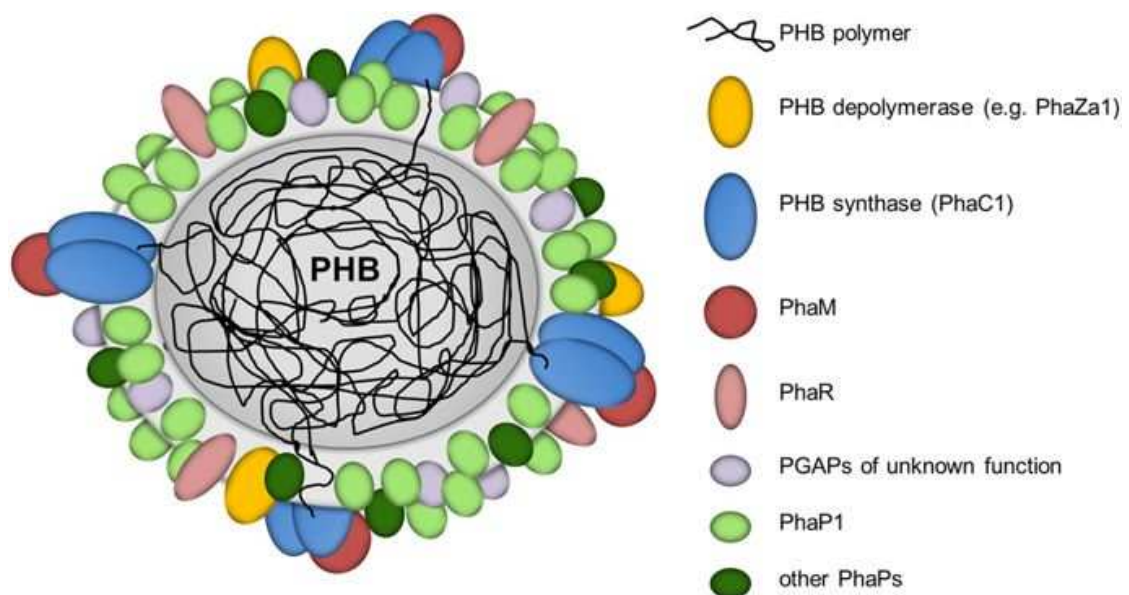


Figure 2.3. Model of an *in vivo* P(3HB) granule in *C. necator* H16
 [Source: (Bresan et al., 2016)]

PHA synthase acts as a key enzyme of PHA synthesis. It is utilized for catalyzing the polymerization of CoA to PHA and free CoA. Based on their subunit composition and substrate specificity, PHA synthases can be categorized into four classes (Figure 2.4). Class I synthases (which are found in *C. necator*) produce scl-PHA and Class II synthases (which are found in *Pseudomonas* spp.) produce mcl-PHA and they both have an average subunit size of 60 to 70 kDa. Class III and class IV PHA synthases consist of two subunits (PhaC/PhaE and PhaC/PhaR, respectively). While Class III synthases were cited in *Allochrochromatium vinosum*, Class IV synthases were mainly narrated in *Bacillus* sp. (Jendrossek, 2009).

Class	Representative organism(s)	Subunits	substrate
I	<i>Cupriavidus necator</i>	PhaC ~ 60-73 kDa	3HA _{scl} -CoA (~C ₃ -C ₅) 4HA _{scl} -CoA 5HA _{scl} -CoA 3MA _{scl} -CoA
II	<i>Pseudomonas aeruginosa</i> <i>Pseudomonas oleovorans</i>	PhaC ~ 60-65 kDa	3HA _{mcl} -CoA (~C ₆ -C ₁₄)
III	<i>Allochrochromatium vinosum</i>	PhaC ~ 40 kDa PhaE ~ 40 kDa	3HA _{scl} -CoA (~C ₃ -C ₅) 3HA _{mcl} -CoA (~C ₆ -C ₈) 4/5HA _{scl} -CoA
IV	<i>Bacillus megaterium</i>	PhaC ~ 40 kDa PhaR ~ 22 kDa	3HA _{scl} -CoA (~C ₃ -C ₅)

Figure 2.4. Classification of PHA synthases
[Source: (Rehm, 2006); Rehm & Steinbüchel, 1999]

2.2.3 Properties of PHA

Three main enzymes are involved in the biosynthesis of P(3HB) as follows (Verlinden et al., 2007);

- a. 3-ketothiolase (PhaA)
- b. Acetoacetyl-CoA reductase (PhaB)
- c. PHA synthase (PhaC)

As previously stated, PHA synthases stand out as the main enzymes that play a very significant role in polymerizing a wide range of HA monomers. There are different varieties of carbon sources. Thus, bacteria fed by these variations in the carbon sources determine the synthesis of PHA with different monomers (Steinbüchel & Schlegel, 1991). The synthesis of PHA by the bacteria depends extremely on the variety of carbon source being fed to them as it will result in producing monomers that are structurally identical to that particular carbon source (Philip et al., 2007). Contrarily, some other unrelated carbon sources could also generate monomers, but these monomers would be so completely different from the initial chemical structure. This difference can be explained from the metabolic pathways functioning in the microorganism. PHA biosynthetic pathways can be partitioned into three distinct pathways (Figure 2.5).

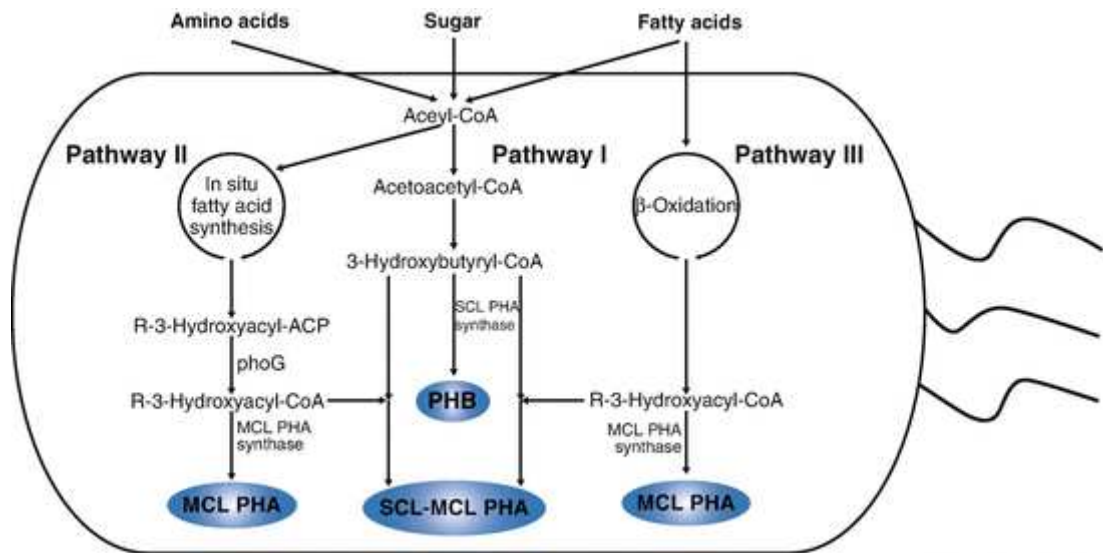


Figure 2.5. PHA biosynthetic pathways in bacteria
[Source: (Chen et al., 2015)]

In Pathway I:

3HB monomers are produced by condensing two acetyl-CoA molecules from the tricarboxylic acid (TCA) cycle resulting in the formation of acetoacetyl-CoA by the enzyme 3-ketothiolase (Senior & Dawes, 1971; Senior & Dawes, 1973). Acetoacetyl-CoA reductase will then act on acetoacetyl-CoA to form 3-hydroxybutyryl-CoA. This in turn will then be polymerized by the PHA synthase to form P(3HB). Pathway I described is used by *C. necator* and most other bacteria that produce P(3HB).

Pathway II:

Also, it is known as fatty acid *de novo* biosynthetic pathway. Carbon sources which are inexpensive, structurally unrelated, and simple are utilized in this pathway to help generate monomers for PHA synthesis. Glucose, sucrose, and fructose are the other sources also being utilized. Rehm et al. (1998) explained that the (*R*)-3-hydroxyacyl intermediates from the fatty acid biosynthetic pathway are transformed

from the form of acyl carrier protein (ACP) to the form of CoA by the enzyme acyl-ACP-CoA transacylase (encoded by *phaG*) (Rehm et al., 1998). This enzyme would then act as the main linker between fatty acid synthesis and PHA biosynthesis.

Pathway III:

This is also known as β -oxidation pathway which deals with enzymes that are associated with fatty acid catabolism or degradation of fatty acids. In this pathway, substrates can be generated if they can be polymerized by the PHA synthases of some pseudomonads. These bacteria have the capability to synthesize mcl-PHA from various alkanes, alkenes, and alkanoates. In *Aeromonas caviae*, the β -oxidation intermediate, trans-2-enoyl-CoA is converted to (*R*)-3-hydroxyacyl-CoA by a (*R*)-specific enoyl-CoA hydratase (Fukui & Doi, 1997; Fukui et al., 1998). The PHA synthases that catalyze the PHA synthesis from fatty acids are responsible for the PHA synthesis from glucose as well (Huijberts et al., 1992).

2.2.4 Types and properties of PHA

Petroleum-based plastics though harmful to environment have been in circulation for a long while. However, PHAs with their appealing properties have gained much attention as an alternative to petroleum-based plastics. The general properties of common types of PHAs are shown in Table 2.1.

Table 2.1. Properties of common types of PHA synthesized by bacteria

Polymer	Melting point (°C)	Young's modulus (GPa)	Tensile strength (MPa)	Elongation to break (%)	Crystallinity (%)	Glass transition temperature (°C)
P(3HB)	180	3.5	40	5	60	4
P(3HB-co-3HV)						
3 mol% 3HV	170	2.9	38	-	-	-
9 mol% 3HV	162	1.9	37	-	-	-
14 mol% 3HV	150	1.5	35	-	-	-
20 mol% 3HV	145	1.2	32	-	-	-
25 mol% 3HV	137	0.7	30	-	40	-1
P(3HB-co-4HB)						
10 mol% 4HB	159	-	24	242	-	-
16 mol% 4HB	130	-	26	444	45	-7
64 mol% 4HB	50	30	17	591	15	-35
78 mol% 4HB	49	-	42	1120	17	-37
82 mol% 4HB	52	-	58	1320	18	-39
90 mol% 4HB	50	100	65	1080	28	-42
P(4HB)	53	149	104	1000	34	-48
P(3HB-co-3HHx)						
5 mol% 3HHx	151	-	-	-	-	0
10 mol% 3HHx	127	-	21	400	-	-1
15 mol% 3HHx	115	-	23	760	-	0
17 mol% 3HHx	120	-	20	850	-	-2
19 mol% 3HHx	111	-	-	-	-	-4
25 mol% 3HHx	52	-	-	-	-	-4
Polypropylene	176	1.7	34.5	400	70	-20
LDPE	130	0.2	10	620	-	-30

[Source: (Khanna & Srivastava, 2005; Kunioka et al., 1989; Saito & Doi, 1994)]

2.3 Poly(3-hydroxybutyrate) [P(3HB)]

P(3HB) homopolymer is characterized as highly crystalline and brittle. Possessing this characteristic makes it unsuitable to be utilized as a plastic material and it is commonly regarded as a PHA with poor mechanical properties. Young's modulus of 3.5 GPa, tensile strength of 43 MPa, and elongation to break at 5% which are extremely low as compared to polypropylene (400%) (Sudesh et al., 2000). The way to improve the properties of the polymer is to incorporate other monomers. In this way, the polymer would become more suitable to be used for different applications.

When P(3HB) polymer is isolated from bacteria, it will usually have a relatively high M_w around 10^6 and will also exhibit a very high crystallinity (Table 2.1). P(3HB) is a stereo regular polyester. The absolute configurations of all the β -carbons in the polymer are identical. This means that the polymer is completely isotactic with its melting temperature around 180 °C. This temperature is just slightly lower than its thermal degradation temperature (185 °C). When the thermal degradation temperature is so close to the melting temperature, it will certainly make the injection molding process difficult.

Table 2.2. General comparison of scl- and mcl-PHA

scl-PHA	mcl-PHA
Stereo regular polyester	Elastomer
Highly crystalline (55-80%)	Low crystallinity (25%)
Stiff and brittle	Flexible and elastic
Melting point (T_m): 173-180 °C	Melting point (T_m): 39-61 °C
Glass transition temperature (T_g): 5-9 °C	Glass transition temperature (T_g): -43 to -25 °C

[Source: Modified from (Możejko-Ciesielska & Kiewisz, 2016)]

Not only P(3HB) has several useful properties such as moisture resistance and water insolubility but it also exhibits good oxygen impermeability (Holmes, 1988). The elongation to break for P(3HB) is only 5% and P(3HB) is much stronger in terms of stiffness when compared with PP; however, it is relatively more brittle.

PHA synthase gene (*phaC*) from *C. necator* expressed in recombinant *Escherichia coli* can produce ultra-high-molecular weight P(3HB) homopolymer ranging from 3×10^6 to 1.1×10^7 (Kusaka et al., 1999). These ultra-high-molecular weight polymers demonstrate much better mechanical properties when compared to those produced by the wild-type bacterium. The ultra-high-molecular weight P(3HB)

possessed elongation to break, Young's Modulus and tensile strength of 58%, 1.1 GPa, and 62 MPa, respectively (Kusaka et al., 1999).

2.4 Poly(3-hydroxybutyrate-co-3-hydroxyhexanoate) [P(3HB-co-3HHx)]

P(3HB-co-3HHx) with the backbone of scl monomer (3HB) and an mcl monomer (3HHx) serves as another interesting polymer. Incorporating 5 mol% 3HHx units into the 3HB sequence has resulted in a reduction in the melting point from 180 to below 155 °C which eventually led to a significant improvement of the thermal and physical properties (Loo et al., 2005). The elongation to break increased from 5 to 400% when 10 mol% 3HHx monomers were incorporated into the 3HB sequences. This makes the polymer more flexible (Sudesh et al., 2000). Therefore, when both scl and mcl are combined, they exhibit a better property of PHA. P(3HB-co-3HHx) stands out as an interesting copolymer.

P(3HB-co-3HHx) copolymer was first discovered in *Aeromonas caviae*. The findings are as follows: 1) The T_m of P(3HB-co-3HHx) decreases from 178 °C to 120 °C once the 3HHx monomer fraction increases from 0 to 17 mol%, and 2) The ΔH_m and T_g also decrease with increasing 3HHx fraction from 97 J/g to 34 J/g and from 4 °C to -2 °C, respectively (Shimamura et al., 1994). In contrast, the elongation at break increases from 5 to 850%. This result shows that the P(3HB-co-3HHx) copolymer will become soft and flexible with an increase in the 3HHx fraction.

2.5 PHA-producing bacteria

Although more than 300 bacterial species can produce PHA, most of them are not able to accumulate high quantity of PHA. *Cupriavidus necator*, *Alcaligenes latus*, *Pseudomonas oleovorans*, *Pseudomonas putida*, recombinant *Escherichia coli*,

and *Azotobacter vinelandii* are some of the bacteria that can produce sufficiently high quantity PHA and on top of that, they can be easily isolated from wastewater, rivers, or soil (Khanna & Srivastava, 2005). Wild-type bacteria, recombinant bacteria, and mixed culture bacteria are the three types of bacteria often used in the synthesis of PHA. Wild-type bacteria can be divided into two groups based on their PHA accumulation pattern: The first group produces PHA under limited essential nutrients such as *Cupriavidus necator*, *Rhodopseudomonas palustris*, and *Methylobacterium organophilum*. The second group of bacteria such as *Alcaligenes latus* and recombinant *Escherichia coli* which contain PHA biosynthetic genes will produce PHA alongside growth in the cultivation medium. This means no limitation of essential nutrients is necessary to induce PHA biosynthesis (Akaraonye et al., 2010). Both these groups are also known as non-growth associated and growth associated PHA producers, respectively.

2.6 *Cupriavidus necator* and its ability to utilize various carbon sources

Cupriavidus necator is a Gram-negative bacterium popularly known as *Alcaligenes eutrophus* and *Ralstonia eutropha*. *C. necator* is a non-obligate bacterial predator of various Gram-negative and Gram-positive soil bacteria and fungi. It also exists as a non-spore forming, rod-shaped, and flagellated bacteria with an oxidative metabolism.

Research report shows that *C. necator* can consume some sugars, plant oil, vegetable oil, and carbon dioxide and accumulate PHA up to 80 wt% of CDW (Tsuge, 2002). Few experiments of P(3HB) production were conducted by using glucose as the sole carbon source within the concentration of 10-20 g/L resulting in the final cell mass of 164 g/L with P(3HB) content of 76 wt% obtained.

Although, as stated earlier in this chapter, plant oils are preferred to be used as feed stocks because they are inexpensive when compared to other carbon sources, it is not available in abundance in every countries. Therefore, an alternative inexpensive and abundant carbon source such as sugar is required to produce PHA.

2.7 Glucose as carbon source for PHA biosynthesis

The beneficial aspect of microorganisms is that they can produce PHA from sugar. Most PHA-producing microorganisms can use simple sugars and glucose is one among them to use in production of PHA. For example, *Pseudomonas* spp. can use glucose and other simple sugars to synthesize medium chain-length PHAs such as poly(3-hydroxyhexanoate) [P(3HHx)] (Haywood et al., 1990, Sun et al., 2007). However, *Ralstonia eutropha* can only synthesize poly(3-hydroxybutyrate) [P(3HB)] by using fructose to better understand the conversion of various substrates (Anderson & Dawes, 1990). Wild-type H16 is deficient in assimilating glucose, a major sugar in non-edible cellulosic resources. For that reason, several glucose-utilizing mutants were constructed by modification of *nag* operon (Mifune et al. 2008; Orita et al. 2012). A few glucose-utilizing mutants of *C. necator* have been isolated by UV and spontaneous mutagenesis (Raberg et al., 2012), and constructed by targeted genetic engineering (Poirier et al., 1992). As an experiment revealed, there was an experimental high-level yield of PHA production from glucose. These high-level yields roughly ranged from 0.3 to 0.4 g P(3HB)/g glucose (Akiyama et al., 2003).

With regards to the point above, the research reports showed that carbon sources such as glucose and fructose along with fatty acids were successfully used to synthesize PHAs copolymer and tercopolymer, and this was carried out by using various bacterial strains (Masood et al., 2017; Ray & Kalia 2017). On top of that,

production of polyester consisting of 3-hydroxybutyric acid (3HB) and of medium-chain-length 3-hydroxyalkanoic acids (3HA) of C6, C8, C10, and C12 by *Pseudomonas* sp. 61-3 (isolated from soil) was investigated when sugars such as glucose, fructose, and mannose were fed as the sole carbon source (Kato et al., 1996). On the other hand, ZENECA Bio products had patented number of PHA production. This was conducted by using *C. necator* strain to produce homopolymer and copolymer by using glucose as the sole carbon source and mixture of glucose and precursors, respectively (Byrom, 1987; Byrom, 1992).

Besides this, Huijberts et al. (1992) carried out studies on *Pseudomonas putida* KT2442 cultivated on glucose to accumulate poly(3-hydroxyalkanoates) consisting of saturated and unsaturated monomers (Huijberts et al., 1992). At the same time, earlier study also mentioned poly- β -hydroxybutyrate biosynthesis and the regulation of glucose metabolism in *Azotobacter beijerinckii* (Senior & Dawes, 1971). In addition, it was noted that statistical physical and nutrient optimization of bioplastic polyhydroxybutyrate production by *C. necator* ATCC 17699 from glucose was obtained from the Persian Type Culture Collection to produce P(3HB) (Aramvash et al., 2015). PHA from glucose is generally synthesized from acetyl-coenzyme A (CoA) by a sequence of three reactions catalyzed by 3-keto-thiolase, NADPH-dependent acetoacetyl-CoA reductase, and PHB synthase as mentioned earlier in Section 2.2.3 referring to Figure 2.5.

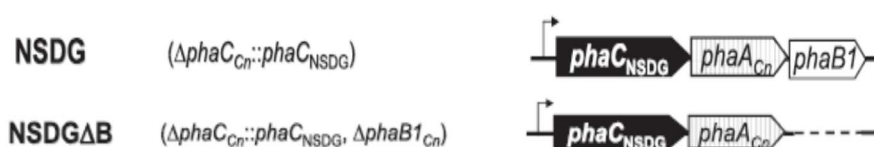
2.8 NSDG and NSDG Δ B1 mutant strains and glucose pathway for P(3HB) and P(3HB-co-3HHx) production

In the last two decades, *C. necator* has been used as a host for functional analyses of PHA-biosynthesis genes and as a platform for molecular breeding aiming

efficient production of PHAs (Fukui et al., 2011). Whole genome information of *C. necator* wild strain H16 has allowed researchers to estimate carbohydrate metabolisms in this bacterium (Orita et al., 2012).

Unfortunately, *C. necator* H16 and the closely related strains cannot grow on glucose, a major sugar in cellulosic materials, leading to limitation of these strains for production of PHAs from non-edible biomass (Orita et al., 2012). In order to achieve effective metabolic engineering of PHA-producing bacteria, the genes for PHA biosynthesis or the related carbon and energy metabolisms should be appropriately expressed or silenced without negative impacts on other cellular functions such as growth ability (Fukui et al., 2011).

The strain NSDG with $\Delta phaC_{Cn}::phaC_{NSDG}$ genotype was constructed from H16 ΔC , and NSDG $\Delta B1$ strain was constructed from NSDG as the parent strain (Orita et al., 2012). *Cupriavidus necator* NSDG-GG and NSDG-GG $\Delta B1$ /pBPP-ccr_{Me}J_{Ac}-emd are glucose-utilizable engineered strains of wild strain H16 which has been constructed from strains NSDG and NSDG $\Delta B1$ by modification of *nag* operon and replacement of *phaC* with a mutant gene of *phaC* derived from *Aeromonas caviae* on the chromosome, respectively (Fukui et al., 2014; Mifune et al. 2008; Orita et al. 2012). The schematic diagrams of *pha* operon in *C. necator* strains used in this study are shown below.



i. Poly(3-hydroxybutyrate) [P(3HB)] pathway by NSDG-GG strain

So far, engineered strains of H16 capable of utilizing glucose were established by expressing glucose facilitator (*glf*) and glucokinase (*glk*) from *Zymomonas mobilis* (Orita et al., 2012) or by reconstituting mutations identified in *nag* operon within the glucose-utilizable mutants (Orita et al., 2012; Raberg et al., 2012).

The genes of the three enzymes for P(3HB) biosynthesis, β -ketothiolase (PhaA), NADPH-dependent acetoacetyl-CoA reductase (PhaB1), and PHA synthase (PhaC1) clustered in the chromosome 1 of *C. necator* as phaC1-A-B1 (Fukui et al., 2011).

Extracellular fructose is possibly transported into the cells by fructose specific ATP-binding cassette (ABC)-type transporter (H16_B1498-B1500), and subsequently converted to glucose-6-phosphate (G6P) by catalytic reactions with fructokinase (H16_B1503) and glucose-6-phosphate isomerase (H16_B1502). G6P then enters Entner-Doudoroff pathway mediated by glucose-6-phosphate (G6P) 1-dehydrogenases (H16_A0316, H16_B1501, and H16_B2566), 6-phosphogluconolactonase (H16_B2565), phosphogluconate dehydratase (H16_B2567), and 2-keto-3-deoxy-6-phosphogluconate aldolase (H16_B1213), to generate pyruvate and glyceraldehyde-3-phosphate. Glucokinase (Glk) or hexokinase then acts on formation of G6P from the imported glucose besides transportation by PTS mediating 6-phosphorylation-associated transportation. Considering the shared metabolisms between fructose and glucose after the formation of G6P, it is feasible that *C. necator* H16 may have deficiency in generation of G6P from extracellular glucose.

Firstly, the deficiency of both uptake and successive phosphorylation of glucose in wild strain H16 was confirmed by heterologous expression of genes for glucose transport and assimilation system from *Z. mobilis*. Then, it identified previously unknown mutation points in the glucose-utilizing mutant *C. necator* NCIMB 11599 and examined to reconstitute the glucose-utilization ability by introducing the identified mutations onto the chromosome 1 of wild strain H16. Then, the mutation in *nagE* and disruption of *nagR* introduced onto chromosome 1 of wild strain H16 by homologous recombination. The resulting engineered strain *C. necator* *nagE_G265RΔnagR* exhibited comparable growth and P(3HB) accumulation on glucose to those of the wild strain on fructose, demonstrating successful reconstitution of functional glucose-uptake and phosphorylation system. This recombinant strain is expected to be useful in further engineering for efficient production of PHAs from inexpensive biomass resources.

Overexpression of *nagE* and *nagFE* from *C. necator* strains H16 and NCIMB 11599 was conducted under the control of a native promoter region for *phaPCJ* in *A. caviae* (P*pha*-Ac). The resulting plasmids for expression of *nagE* from *C. necator* H16 and NCIMB11599, and *nagFE* from *C. necator* H16 and NCIMB 11599 were designated pBPHAc-*nagEH16*, pBPHAc-*nagE11599*, pBPHAc-*nagFEH16*, and pBPHAc-*nagFE11599*, respectively.

It successfully reconstituted the glucose-utilization ability in *C. necator* wild strain H16 by using homologous recombination based on the new finding that Gly265Arg mutation in NagE and derepression of *nagFE* by loss of NagR function are necessary and sufficient factors for glucose assimilation by the mutant strain NCIMB 11599. Moreover, this strain is plasmid-free, therefore additional genetic modifications can be easily examined by transformation with single plasmid. This is

an advantage of this strain over the previously reported strain already harboring one plasmid for glucose assimilation because the introduction of multiple plasmids often causes growth inhibition and instability of the resulting transformant. The strain reconstituted is expected to be a useful platform for tailor-made engineering aimed at efficient production of P(3HB-*co*-3HHx) copolymers with superior physical properties from inexpensive biomass resources (Fukui et al., 2014; Orita et al., 2012).

ii. Poly(3-hydroxybutyrate-*co*-3-hydroxyhexanoate) [P(3HB-*co*-3HHx)] pathway by NSDG-GG Δ B1/pBPP-*ccr*_{MeJ_{Ac}}-*emd* strain

PHA synthase gene derived from *A. caviae* on the H16C_{Ac} chromosome was replaced by a gene encoding the N149S/D171G mutant and this recombination enhanced PHA productivity as well as slightly increased 3HHx composition. It was firstly applied a mutant enzyme of *PhaC*_{Ac} (*PhaC*_{NSDG}), previously obtained by *in vitro* evolution for the chromosomal engineering of *C. necator*. Next, deletion of *phaA*_{Cn}/*phaB1*_{Cn} and insertion of *bktB*_{Cn}/*phaJ*_{Ac} were performed within *pha* operon on the chromosome of *C. necator* to depress 3HB monomer supply and promote 3HHx monomer supply through β -oxidation, respectively (Mifune et al., 2010).

The engineered strain of *C. necator* with Δ *phaB1* genotype expressing *ccr*, *phaJ4a*, and *emd* could produce P(3HB-*co*-3HHx) from fructose. Depression of (*R*)-specific reduction of acetoacetyl-CoA by the deletion of *phaB1* was an effective modification for formation of the C6–monomer unit from fructose driven by crotonyl-CoA carboxylase/reductase (*Ccr*). When this pathway was installed into *C. necator* strain PHB⁻4, the resulting recombinant strain accumulated P(3HB-*co*-3HHx) from fructose. The results demonstrated that the lack of *PhaB1* was particularly important for the *Ccr*-driven formation of (*R*)-3HHx-CoA from fructose

in *C. necator* (Insomphun et al., 2015). Subsequently, the engineered NSDGΔB1 strain was constructed with deletion of *phaB1*_{Cn} and harboring pBPP by integrating additional two modification for glucose assimilation and enhanced glycerol assimilation to produce P(3HB-co-3HHx) (Fukui et al., 2014). *Ralstonia eutropha* strains capable of synthesizing P(3HB-co-3HHx) from not only fructose but also glucose and glycerol were constructed by integrating previously established engineering strategies. Further modifications were made at the acetoacetyl-CoA reduction step determining flux distribution responsible for the copolymer composition. When the major acetoacetyl-CoA reductase (PhaB1) was replaced by a low-activity paralog (PhaB2) or enzymes for reverse β -oxidation, copolyesters with high 3HHx composition were efficiently synthesized from glucose, possibly due to enhanced formation of butyryl-CoA from acetoacetyl-CoA via (S)-3HB-CoA.

2.9 Central Composite Design (CCD) and Response Surface Methodology (RSM)

In the quantitative optimization of bioprocess, a robust design of experiment (DOE) needs to be fabricated so that the input parameter levels and their interaction can be analyzed. Besides this, the aim of statistical optimization experiment is to construct a predictive statistical mathematical model. This is to predict the behavior of the process being investigated. They create the graphical statistical models which can be obtained from RSM (Montgomery, 2017). CCD has become the most popular design for RSM used to fit models determined. It is usually called a CCD but in fact it is just a Box-Wilson central composite design. In close examination, we notice that this design consists of a factorial design (FD) fitted with center points and rotating points (star or axial points) that allow estimation of curvature and generate a second-